Kinetics of thin-film reactions of Cu/*a*-Ge bilayers

Z. Wang, G. Ramanath, L. H. Allen, and A. Rockett[a)]
Coordinated Science Laboratory, Materials Research Laboratory, and Department of Materials Science and Engineering, University of Illinois at Urbana-Champaign, 1101 West Springfield Avenue, Urbana, Illinois 61801

J. P. Doyle and B. G. Svensson
Royal Institute of Technology, Solid State Electronics, P.O. Box E229, S-164 40 Kista-Stockholm, Sweden

(Received 22 July 1996; accepted for publication 24 June 1997)

The kinetics of the Cu_3Ge phase formation during reactions between 600 nm polycrystalline Cu (poly-Cu) and 600 nm amorphous Ge (*a*-Ge) layers on Si (100) substrates have been studied as a function of annealing conditions. Monoclinic Cu_3Ge nucleated rapidly, resulting in smooth Cu_3Ge layers. The room-temperature resistivity of the Cu_3Ge was $\sim 8\ \mu\Omega$ cm ($\sim$4.5 times that of pure Cu). The real-time resistance versus temperature $[R(T)]$ characteristics were nearly identical for heating rates of 0.1–5 °C/min. Modeling of the $R(T)$ data indicates that the reaction was predominantly diffusion controlled with a rate of $(4\times10^{-3}\ \mathrm{cm^2/s})\ \exp\ [-0.85\pm0.01\ \mathrm{eV}/kT]$ where $k=8.617\times10^{-5}$ eV/K. Secondary ion mass spectrometry profiles and $R(T)$ data for the films annealed to various temperatures indicate that the Cu_3Ge/Ge interface is stable for $T<300$ °C. © *1997 American Institute of Physics.* [S0021-8979(97)02619-4]

I. INTRODUCTION

Copper, with its low electrical resistivity and stability against void formation and electromigration, has long been suggested as a replacement for Al in microelectronic interconnects and contacts.[1] Recently, there has been a major effort to integrate Cu metallizations in Si-based ultra-large-scale integrated circuits.[2,3] Direct contact between Cu and Si generally yields copper silicides. It has been found that impurities play an important role in determining the copper silicide reaction kinetics[4–6] and resulting electrical properties.[7,8] Cu silicides also exhibit rapid oxidation in air.[9] These behaviors have made Cu metallizations on Si relatively unattractive. However, preliminary results have recently suggested that Cu germanides may provide superior performances.[10]

A recent study has shown that the formation of Cu_3Ge on Si (100) at 200 °C produced no deep level states in the Si due to Cu.[10] In addition, Cu germanides, unlike Cu silicides, are relatively oxidation resistant. Further, recent advances in Si–Ge heterojunction devices have stimulated renewed interest in contacts compatible with Ge and Si–Ge alloys.[11] It has been found that Cu_3Ge exhibits unexpectedly low electrical resistivities at room temperature[12] and is believed to be the only phase formed in thin-film reactions between Cu and Ge.[5,13] Unlike the silicides, which have been widely studied,[14] the literature on germanides is very limited.[15–17] These considerations make reactions of Cu with Ge a topic of current interest. For the copper germanide system, most of the studies, thus far, have concentrated on phase formation in Cu–Ge thin-film[5,13] and bulk[18] diffusion couples. However, the thin-film reaction kinetics remain to be demonstrated.

In this work, a detailed characterization of the diffusion behavior, phase formation, and kinetics of thin-film reactions between 600 nm polycrystalline Cu (poly-Cu) and 600 nm of amorphous Ge (*a*-Ge) films is presented as a function of annealing conditions.

II. EXPERIMENTAL PROCEDURE

The Cu/*a*-Ge samples were grown by sequential electron-beam evaporation of Ge and Cu on hydrogen-terminated or thermally oxidized Si (100) substrates in a system with a base pressure of $\sim 7\times10^{-6}$ Pa (5×10^{-8} Torr). Prior to the deposition, the unoxidized silicon substrates were degreased with solvents and then dipped in a 10% HF solution in deionized water and pulled dry. The deposition rate was 0.4 nm/s for both the Ge and Cu layers. After deposition, the samples were stored in a dry nitrogen environment.

The samples were annealed in a high-vacuum furnace with base pressure of 3×10^{-6} Pa (2×10^{-8} Torr) and equipped with a four-point spring-loaded probe assembly in a van der Pauw configuration.[19,20] Probes were located near the corners of the rectangular 7 mm × 9 mm samples. The interprobe separation was much larger than the film thickness and a fixed geometry of the probes and a uniform sample size and shape were preserved from run to run. The resistance, $R=V/I\ (\Omega)$, was calibrated against a sample of unreacted Cu on SiO_2 before each anneal. Annealing treatments were carried out under either controlled-rate heating or isothermal conditions and the resistance of the film was monitored *in situ* during the experiments. After the anneal, the samples were quenched to room temperature and examined by a number of techniques to correlate the physical characteristics with the resistance measurements.

Cross-sectional transmission electron microscopy (XTEM) experiments were conducted in Philips 420 or CM12 TEMs. These microscopes are equipped with energy-dispersive x-ray spectroscopy (EDXS) for *in situ* chemical composition analysis. The beam voltage was 120 kV. Specimens were prepared by cutting samples into two pieces and

a)Electronic mail: arockett@staff.uiuc.edu

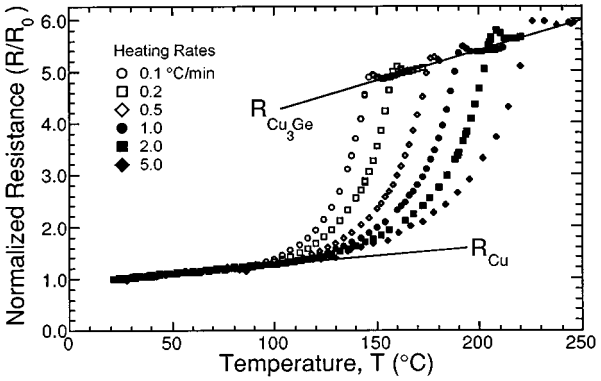

FIG. 1. Normalized resistance versus temperature data at various ramp rates for 600 nm Cu on 600 nm Ge on a Si substrate. Straight lines indicate the fit temperature-dependent resistances for the Cu and Cu_3Ge layers. Values for R_0 are given in Table I.

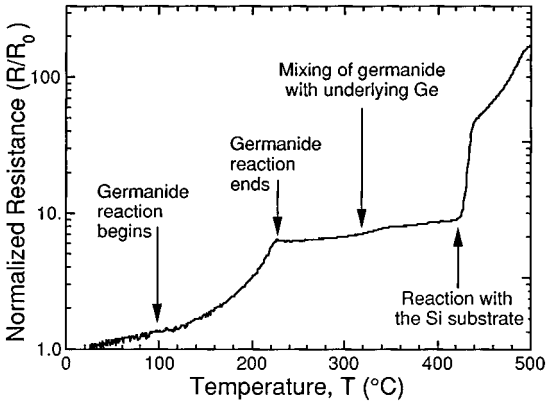

FIG. 2. Normalized resistance versus temperature during a temperature ramp at a rate of 5 °C/min from room temperature to 500 °C for Cu and a-Ge films on an unoxidized Si substrate. Films on oxidized substrates behaved similarly but did not show the abrupt increase in resistance at ~430 °C.

gluing them together face to face. This sandwich was then cleaved into slabs ~300 μm thick and thinned by mechanical grinding and polishing down to a few tens of microns. The specimen was then mounted on a copper ring and ion milled on both sides to electron transparency. Ion milling was carried out in a Gatan Model 600 ion miller using two 6 kV, 5 mA Ar^+-ion beams incident at 12° to the sample surface on a liquid-nitrogen-cooled stage.

X-ray diffraction (XRD) experiments were carried out using a Rigaku D-Max III powder diffractometer equipped with a monochromatic Cu $K\alpha$ radiation source. The positions of the x-ray peaks were calibrated by aligning the diffractometer to the Si (400) substrate peak. Compositional depth profiles were obtained by secondary ion mass spectrometry (SIMS) in a Cameca IMS-5f instrument using a 10 keV Cs^+ primary ion beam.

III. RESULTS

Figure 1 shows the variation of resistance R of 600 nm of Cu on 600 nm of a-Ge on an oxidized Si wafer for films annealed under temperatures T increased at rates dT/dt of 0.1, 0.2, 0.5, 1, 2, and 5 °C/min. The similarity of these curves suggests the same basic reaction path for all heating rates studied. The resistance behavior for the 5 °C/min ramp over a wider temperature range is shown in Fig. 2. Similar high-temperature results were obtained at other heating rates. The basic behavior can be summarized as follows: From room temperature to ~100 °C, the resistance increased linearly with T to ~0.01 Ω and then increased rapidly as the reaction occurred. The reaction was complete by 230 °C. The resistance decreased slightly upon completion of the reaction. This was followed by a linear resistance increase to ~320 °C. Between ~320 and ~350 °C, the slope changed, while above 430 °C the resistance increased rapidly. Comparison of $R(T)$ results for Cu/Ge/Si and Cu/Ge/SiO_2/Si configurations with 600 nm Cu and 600 nm Ge in each case showed identical behavior to 430 °C,[21] indicating no reaction with and negligible electrical conduction through the Si substrate. Above 430 °C, the films on the unoxidized wafers reacted with the Si. The temperature at which the Cu_3Ge phase formed was a function of the heating rate, increasing as the heating rate increased.

Bright-field XTEM micrographs are shown in Figs. 3(a) and 3(b) of films heated to 115 and 240 °C, respectively, at a heating rate of 2 °C/min and then cooled rapidly to room temperature. It is evident from Fig. 3(a) that a thin layer of Cu_3Ge with flat interfaces formed between the Cu and the Ge, indicating that the reaction process is not nucleation limited even at low temperatures.[22] For the film annealed to 240 °C, convergent beam diffraction patterns [Fig. 3] and micro-EDXS showed the presence of a 760 nm thick polycrystalline Cu_3Ge layer with grain sizes from ~0.1 to ~0.5 μm, averaging ~0.2 μm. Beneath the Cu_3Ge is an ~230 nm thick microcrystalline Ge layer. It is interesting to note that the a-Ge crystallized at much lower temperatures in the presence of the germanide than is observed for a-Ge layers alone. This reduction in crystallization temperature is consistent with previous observations of silicide-mediated crystallization of amorphous Si.[23] It has been suggested previously that this may be the result of the presence of copper.[15] Hong *et al.* found that the interface between the amorphous germanium and the gemanide was a nucleation center for crystallization of a-Ge. It was also suggested that the Cu_3Ge nucleated between the Cu and polycrystalline germanium.[5] However, the crystallization of the a-Ge near the Cu_3Ge interface was not observed in the initial stage of the Cu_3Ge phase formation in the present study [see Fig. 3(a)]. Analyses of convergent beam diffraction patterns [Fig. 3(d)] and XRD peak positions for the sample annealed to 240 °C were consistent with monoclinic Cu_3Ge (Ref. 24) ($a=0.2631$ nm, $b=0.4200$ nm, $c=0.4568$ nm, and $\beta=89.68°$) in agreement with previous works.[13,25] The final germanide thickness based on Cu_3Ge with a molar volume of 30.44 cm^3/mol (Ref. 26) and molar volumes of Cu and Ge of 8.08 and 13.64 cm^3/mol, respectively, was estimated to be 760 nm after consumption of all of the Cu; in excellent agreement with the above result.

Figure 4 shows SIMS depth profiles for the unreacted structure and after heating to 120, 210, and 300 °C. The Cu-

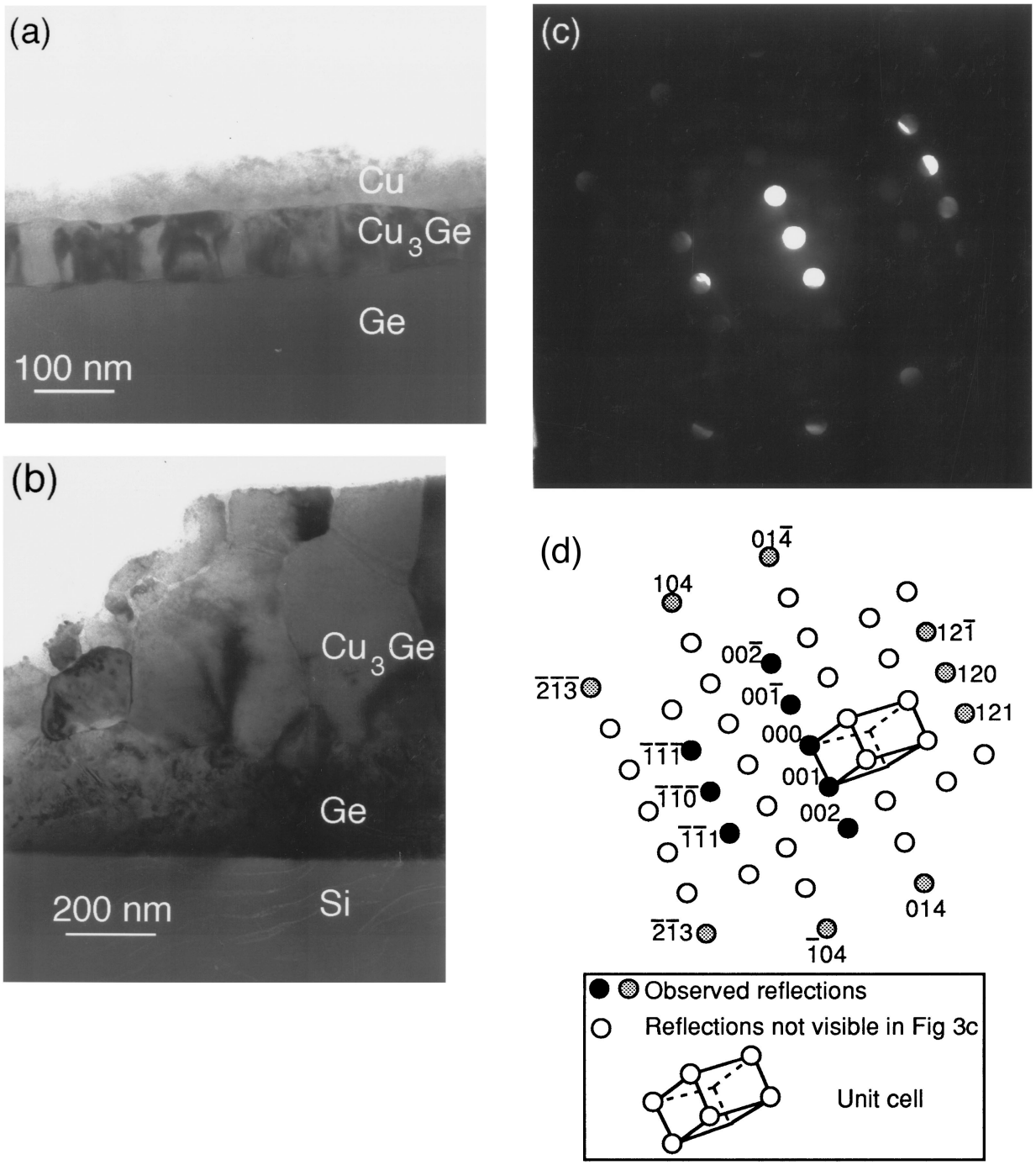

FIG. 3. Bright-field XTEM micrographs of films annealed to (a) 115 °C and (b) 240 °C heated at a rate of 2 °C/min. (c) A convergent beam diffraction pattern obtained near the [110] zone axis. (d) presents a simulation of the diffraction pattern in (c). In the simulation, the black circles are diffraction points in the zero-order Laue zone, while gray circles mark the first-order zone reflections. Open circles show reflections for which diffraction conditions prevented significant intensity. The diffraction points are indexed for the monoclinic Cu_3Ge phase. No other phase provides an acceptable fit to the pattern.

to-Ge count ratio in the germanide was found to be constant in the germanide regions, indicating the growth of a new phase with a fixed stoichiometry and abrupt interfaces, as expected from the TEM work. Between ~320 and ~350 °C, mixing of the Cu_3Ge and residual Ge was found, in agreement with previous results.[12,16] Ge rich Cu_3Ge has also been observed in bulk materials, resulting in alteration of the crystal structure as well as electrical resistance.[25] At ~430 °C, Si diffused through the germanide to the surface and caused a drastic change in the overall resistivity of the multilayer for samples on unoxidized wafers.

IV. REACTION KINETICS ANALYSIS

To quantify the above results, the $R(T)$ data in Fig. 1 were modeled using a three-layer parallel resistor model.[27] The Cu, Cu_3Ge, and Ge layers were assumed to be simple resistors with the resistance of each phase scaling linearly

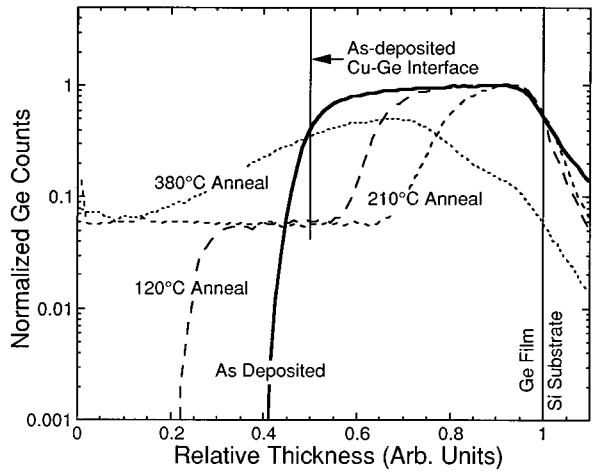

FIG. 4. Ge secondary ion depth profiles for as-deposited films and films annealed to 120, 210, 300, and 380 °C. Cu and Si profiles were recorded simultaneously but are not shown to simplify the figure.

with the layer thickness. In all cases, the Ge was not found to contribute significantly to conduction in the structure, hence, effectively a two-layer parallel resistor model sufficed.

Figure 5 shows a detailed $R(T)$ result for a sample annealed to 285 °C at a heating rate of 1 °C/min. Since before the reaction the majority of the current flows through the Cu, the initial linear increase of the resistance is due to the temperature variation of the resistance of the Cu. A similar argument applies to the linear resistance change after the reaction is complete (230–320 °C), which indicates the temperature coefficient of the Cu_3Ge resistance. Thus, the first step in modeling the data was to account for the linear resistance of the initial and final phases. Assuming a standard parallel-resistor equivalent circuit,

$$R(T)^{-1}=\left(R^0_{\mathrm{Cu}}+T\,\frac{dR_{\mathrm{Cu}}}{dT}\right)^{-1}[1-x(T)]+\left(R^0_{CG}+T\frac{dR_{CG}}{dT}\right)^{-1}\times(T), \tag{1}$$

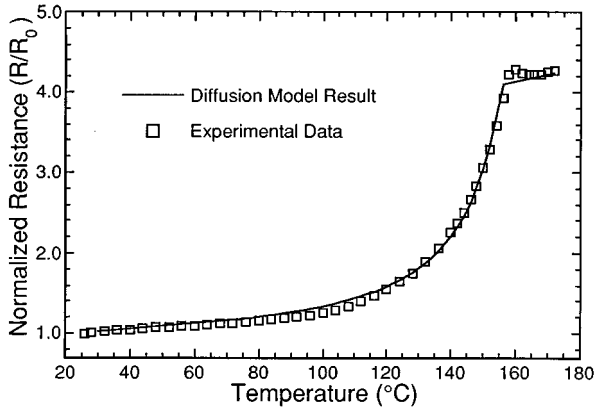

FIG. 5. Experimental data shown in Fig. 1 for a ramp rate of 0.2 °C/min along with fitting results. Similar fits were obtained for the other heating rates measured, although at the highest heating rates, the fit curves fell slightly below the data toward the end of the reaction.

where $x(T)$ is the normalized germanide thickness, and the room-temperature resistances and the rates of change of resistance with temperature for the Cu and Cu_3Ge layers are R^0_{Cu} and R^0_{CG}, and dR_{Cu}/dT and dR_{CG}/dT, respectively. $x(T)=0$ before the reaction and $x(T)=1$ after the reaction is complete. From fitting the curves in Fig. 1, the following values were obtained: $R^0_{\mathrm{Cu}}=0.007\,33\,\Omega$ at 0 °C, $dR_{\mathrm{Cu}}/dT=2.94\times10^{-5}\,\Omega/°\mathrm{C}$ [0.68 $\mu\Omega$ cm/K], $R^0_{CG}=0.0247\,\Omega$ [8 $\mu\Omega$ cm], and $dR_{CG}/dT=9.23\times10^{-5}\,\Omega/°\mathrm{C}$ [1.5 $\mu\Omega$ cm/K], in good agreement with previous measurements for Cu (Ref. 28) and Cu_3Ge.[12]

Based on the observation of smooth interfaces on both sides of the germanide, it was initially assumed that the nucleation rate was high for all temperatures considered. Assuming no nucleation-rate-limited regime, a standard equation[22] for the germanide thickness $x(T)$ was used to describe the reaction

$$\frac{dx(T)}{dt}=\frac{D(C/N)k_s}{D+k_sx(T)}, \tag{2}$$

where D is the diffusivity of the moving species (assumed here to be Cu) and is presumed to be of the general form $D_0e^{-Q/kT}$, where D_0 is a constant, k is Boltzmann's constant, and Q is the diffusion activation energy; C and N denote the concentration of reactant and number of product species per unit volume, respectively; k_s is the reaction rate constant; and t is the heating time. In general, reaction or diffusion rates dominate in the early and late stages of the reaction, respectively. If we assume that the reaction is diffusion rate limited, Eq. (2) can be simplified by assuming $k_sx(T)\gg D$ to

$$dx(T)=2D(C/N)dt=2Ddt. \tag{3}$$

We have no data to make a quantitative estimate of C/N, and so, this was taken as unity for the current calculations. If the assumption of $C/N=1$ is inaccurate, then the value of D_0 in Eq. (4) is modified by a similar factor. From Eq. (3),

$$x^2(T)=\int_{273}^{T}D_0e^{-Q/kT}\,\frac{dt}{dT}\,dT=\frac{2D_0}{r}\int_{273}^{T}e^{-Q/kT}dT. \tag{4}$$

Similar equations were developed for the reaction-rate-limited case [$D\gg k_s$].

Equation (4) was numerically integrated using the MATHEMATICA software package to yield $x(T)$. This was then substituted into Eq. (1) to fit the portion of the curve in which the reaction occurred. The complete fit for the 0.2 °C/min heating rate curve is shown in Fig. 5, and the resulting values for D_0 and Q are given in Table I. Changing the value of D_0 was found to translate the fit curve along the temperature axis while changes in Q changed the shape of the curve. This behavior makes alternate fits for Q and D_0 significantly poorer in comparison to the results presented here. The value of Q is very stable from run to run, although some variation in D_0 was observed. Minor variations in the room-temperature resistivity of Cu_3Ge were also observed in the best fits, probably due to changes in the Cu_3Ge microstructure as a function of the heating rate. The variation in D_0 probably resulted from changes in the effective reaction-rate

TABLE I. Results obtained from fitting experimental $R(T)$ data for various heating rates.

Heating rate dT/dt (°C/min)	Energy Q (eV)	Constant $D_0(\times 10^{-3}$ cm^2/s)	Initial resistance R_0 (Ω)
0.1	0.84±0.02	4.0±1.0	0.005
0.2	0.84±0.02	4.2±1.0	0.007
0.5	0.85±0.02	5.0±1.0	0.008
1.0	0.85±0.02	4.0±1.0	0.005
2.0	0.85±0.02	3.8±1.0	0.008
5.0	0.86±0.02	5.0±1.0	0.003

constant with the heating rate. The quality of the fits at higher heating rates was significantly worse in the estimation of the final film resistance than at lower rates.

It is possible that the reaction includes a reaction-rate-limited regime in addition to the diffusion rate behavior described above. To test this possibility, equations similar to Eqs. (3) and (4) were developed assuming an entirely reaction-rate-limited behavior, and new fits focusing on the lower temperature portion of the $R(T)$ curves were attempted. In addition, a model incorporating both mechanisms was considered. However, no acceptable or consistent fits were obtained. A similar test was made to determine if nucleation was likely to limit the process at low temperature, which yielded equally poor results. It was concluded that for all of the heating rates studied, and over all temperatures where a reaction was detectable by $R(T)$ measurements, the reaction was primarily diffusion limited.

A previous study fit only a single point on the $R(T)$ curve where approximately half of the metal thickness had been consumed.[29,30] A similar approach was used here as well, and was found to yield an activation energy for diffusion similar to the average of values given in Table I. However, the value of the activation energy from this simplified method was found to vary according to the fit fraction of Cu consumed. Hence, it was concluded that fitting the entire $R(T)$ curve is worth the additional effort.

V. DISCUSSION

The diffusion rate was found to have an average activation energy of 0.85±0.01 eV and a preexponential factor $D_0 = 4.3 \pm 0.5 \times 10^{-3}$ cm^2/s, although the D_0 value may have been affected by errors in the $C/N=1$ assumption. An Arrhenius plot of diffusion results for bulk,[18] lateral,[5] and thin-film (this work) diffusion couples is presented in Fig. 6. The activation energy of 0.85 eV/atom is ~0.1 eV lower than that reported by Hong *et al.* in their study of lateral diffusion of Cu–Ge couples[5] and ~0.2 eV lower than the bulk diffusion result obtained by Betch *et al.*.[18] The higher activation energy in the bulk diffusion couple probably results from the larger grain sizes (~100 μm) in that study.[17,18] This also suggests that diffusion in the present study was primarily along grain boundaries, based on the activation energy being <1 eV. Overall agreement with these previous works is excellent, indicating that the thin-film couple behaves in a manner analogous to that of a bulk couple.

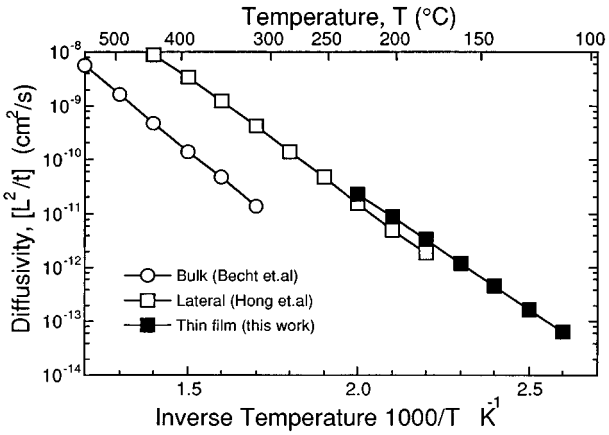

FIG. 6. Comparison of diffusion in bulk (open circles), (see Ref. 18) lateral thin-film (open squares), (see Ref. 5) and stacked thin-film (this work, solid squares) couples.

The absence of a significant nucleation or reaction-rate-limited regime indicates that both of these processes are rapid. This behavior results in excellent germanide morphologies. These features make the Cu germanides attractive as potential contact materials.

VI. CONCLUSIONS

Cu thin films have been found to react in a controlled manner with amorphous Ge layers to produce polycrystalline Cu_3Ge thin films. The morphology of the films is excellent, resulting in highly planar germanide layers. The reactions are diffusion limited over the entire range of conditions studied here. Diffusion activation energies and prefactors agree well with previous studies of bulk diffusion couples.

ACKNOWLEDGMENTS

Two of the authors, J.P.D. and B.G.S., gratefully acknowledge the financial support of the Swedish Board for Technical Development (NUTEK). Two of the authors, Z.W. and A.R., are grateful to the support from the Department of Energy under Contract No. DEFG02-91ER45439. The work using cross-sectional scanning electron microscopy, XRD, SIMS, and XTEM was carried out in the center for Microanalysis of Materials, University of Illinois, which is supported by the U.S. Department of Energy under Grant No. DEFG02-91-ER45439. The assistance of Dr. Jiangang Chen with the transmission electron microscope is also appreciated.

[1] H. Takasago, K. Adachi, and M. Takada, J. Electron. Mater. **18**, 319 (1989).
[2] J. Li, R. Blener, and J. W. Mayer, MRS Bull. **6**, 18 (1993).
[3] J. Li, T. E. Seidel, and J. W. Mayer, MRS Bull. **8**, 15 (1994).
[4] J. G. M. Becht, F. J. J Van Loo, and R. Metselaar, React. Solids **6**, 45 (1988).
[5] S. Q. Hong, C. M. Comrie, S. W. Russell, and J. W. Mayer, J. Appl. Phys. **70**, 3655 (1991).
[6] M. O. Aboelfotoh and L. Krusin-Elbaum, J. Appl. Phys. **70**, 3382 (1991).
[7] S. M. Sze, *Physics of Semiconductor Devices* (Wiley, New York, 1981), p. 21.
[8] A. Cros, M. O. Aboelfotoh, and K. N. Tu, J. Appl. Phys. **67**, 3328 (1990).

[9] J. M. E. Harper, A. Charai, L. Stolt, F. M. d'heurle, and P. M. Fryer, Appl. Phys. Lett. **56**, 2519 (1990).
[10] J. P. Doyle, B. G. Svensson, and M. O. Aboelfotoh (unpublished).
[11] See, for example. G. L. Patton, J. H. Comfort, B. S. Meyerson, E. F. Crabbé, G. J. Scilla, E. D. Defrésar, J. M. C. Stork, J. Y.-C. Sun, D. L. Harame, and J. Burghartz, IEEE Electron Device Lett. **11**, 171 (1990).
[12] L. Krusin-Elbaum and M. O. Aboelfotoh, Appl. Phys. Lett. **58**, 1341 (1991).
[13] F. M. d'Heurle and J. Gupta, Appl. Surf. Sci. **73**, 214 (1993).
[14] M. Nicolet and S. S. Lau, in *VLSI Electronics*, edited by N. G. Einspruch and G. B. Larrabee (Academic, New York, 1983), Vol. 6, p. 329.
[15] J. P. Doyle, B. G. Svensson, M. O. Aboelfotoh, and S. Johansson, Appl. Phys. Lett. **67**, 2804 (1995).
[16] J. P. Doyal, B. G. Svensson, M. O. Aboelfotoh, and J. Hudner, Phys. Scri. **T54**, 297 (1994).
[17] F. M. d'Heurle and P. Gas, J. Mater. Res. **1**, 205 (1986).
[18] J. G. M. Becht, F. J. J. van Loo, and R. Metselaar, React. Solids **6**, 61 (1988).
[19] L. J. van der Pauw, Philips Res. Rep. **13**, 1 (1958).
[20] L. H. Allen, Ph.D. thesis, Cornell University (1990).
[21] Z. Wang (unpublished).
[22] J. W. Mayer and S. S. Lau, *Electronic Materials Science for Integrated Circuits in Si and GaAs* (Macmillan, New York, 1990), p. 311.
[23] C. Hayzelden and J. L. Batstone, J. Appl. Phys. **73**, 8279 (1993).
[24] *Inorganic Index to Powder Diffraction File* (Joint Committee on Powder Diffraction Standards, Pennsylvania, 1995), card numbers 6–693.
[25] M. O. Aboelfotoh and H. M. Tavancy, J. Appl. Phys. **75**, 2441 (1994).
[26] G. F. Baston, F. J. J. van Loo, and H. J. M. Heijligers, X-Ray Spectrom. **13**, 91 (1984).
[27] L. H. Allen, J. W. Mayer, K. N. Tu, and L. C. Feldman, Phys. Rev. B **41**, 8213 (1990).
[28] *CRC Handbook of Chemistry and Physics*, 71st ed., edited by D. R. Lide (Chemical Rubber, Boca Raton, 1990).
[29] K. P. Rodbell, K. N. Tu, W. A. Lanford, and X. S. Guo, Phys. Rev. B **43**, 1422 (1991).
[30] K. N. Tu, J. W. Mayer, and L. C. Feldman, *Electronic Thin Film Science for Electrical Engineers and Materials Scientists* (Macmillan, New York, 1992), p. 331.